

Strategic Latency Reduction in Blockchain Peer-to-Peer Networks

Weizhao Tang
Carnegie Mellon University and IC3

Giulia Fanti
Carnegie Mellon University and IC3

Lucianna Kiffer
Northeastern University

Ari Juels*
Cornell Tech, IC3, and Chainlink Labs

ABSTRACT

Most permissionless blockchain networks run on peer-to-peer (P2P) networks, which offer flexibility and decentralization at the expense of performance (e.g., network latency). Historically, this tradeoff has not been a bottleneck for most blockchains. However, an emerging host of blockchain-based applications (e.g., decentralized finance) are increasingly sensitive to latency; users who can reduce their network latency relative to other users can accrue (sometimes significant) financial gains.

In this work, we initiate the study of strategic latency reduction in blockchain P2P networks. We first define two classes of latency that are of interest in blockchain applications. We then show empirically that a strategic agent who controls only their local peering decisions can manipulate both types of latency, achieving 60% of the global latency gains provided by the centralized, paid service bloXroute, or, in targeted scenarios, comparable gains. Finally, we show that our results are not due to the poor design of existing P2P networks. Under a simple network model, we theoretically prove that an adversary can always manipulate the P2P network’s latency to their advantage, provided the network experiences sufficient peer churn and transaction activity.

CCS CONCEPTS

• **Security and privacy** → *Network security*; • **Networks** → *Network measurement*; **Network algorithms**;

KEYWORDS

blockchains, P2P networks, strategic manipulation

1 INTRODUCTION

Most permissionless blockchains today run on peer-to-peer (P2P) communication networks, which offer the advantages of flexibility and an inherently distributed nature [17, 27]. These benefits of P2P networks typically come at the expense of network performance, particularly the latency of message delivery [16, 17, 39]. Historically, this has not been a bottleneck because most permissionless blockchains are currently performance-limited not by network latency, but by the rate of block production and transaction confirmation, both of which are dictated by the underlying consensus mechanism [12, 16, 20, 26, 44]. For this reason, network latency has not traditionally been a first-order concern in blockchain P2P networks, except where substantial latency on the order of many seconds or even minutes raises the risk of forking [14].

Emerging concerns in blockchain systems, however, are beginning to highlight the importance of *variations in fine-grained network latency*—e.g., on the order of milliseconds—among nodes in blockchain P2P networks. These concerns are largely independent of the underlying consensus mechanism. They revolve instead around strategic behaviors that arise particularly in smart-contract-enabled blockchains, such as Ethereum, where decentralized finance (DeFi) applications create timing-based opportunities for financial gain. Key examples of such opportunities include:

- **Arbitrage:** Many blockchain systems offer highly profitable opportunities for *arbitrage*, in which assets are strategically sold and bought at different prices on different markets (or at different times) to take advantage of price differences [28]. Such arbitrage can involve trading one cryptocurrency for another, buying / selling mispriced non-fungible tokens (NFTs), etc., on blockchains and/or in centralized cryptocurrency exchanges. Strategic agents performing arbitrage can obtain an important advantage through low latency access to blockchain transactions.
- **Strategic transaction ordering:** Blockchains differ from traditional financial systems in their unprecedented transparency and their introduction of new mechanisms for influencing the ordering of transactions. As a result, strategic agents can and do profit from placement of their transactions in ways that exploit / victimize other users—a phenomenon often referred to as *Miner-Extractable Value* (MEV) [10, 15]. For example, strategic agents may *front-run* other users’ transactions, i.e., execute strategic transactions immediately before those of victims, or *back-run* key transactions—e.g., oracle report delivery or token sales—to gain priority when important trading opportunities arise.

Small reductions in network latency can advantage a strategic agent performing such exploits by enabling it to observe victims’ transactions before competing strategic agents do.

- **Improved block composition:** Miners (or validators) rely principally on P2P networks to observe user transactions, which they then include in the blocks they produce. Which transactions a miner includes in a block determines the fees it receives and thus its profits. Therefore the lower the latency a miner experiences in obtaining new transactions, the higher its potential profit.¹
- **Targeted attacks:** The security of nodes in blockchain P2P networks may be weakened or compromised by adversaries’ discovery of their IP addresses. For example, a node may issue critical transactions that update asset prices in a DeFi smart contract. Discovery of its IP address could result in denial-of-service (DoS)

¹Receiving blocks from other miners quickly is also beneficial. To reduce forking risks, however, miners or validators often bypass P2P networks and instead use cut-through networks to communicate blocks to one another [8].

*This work was performed in the author’s Chainlink Labs role.

attacks against it. Similarly, a user who uses her own node to issue transactions that suggest possession of a large amount of cryptocurrency could be victimized by targeted cyberattacks should her IP address be revealed.

As we show in this work, small differences in network latencies in a victim’s transactions can help an adversary distinguish shorter from longer paths to that victim—and with some probability ultimately discover the victim’s IP address.

There is a strong incentive, therefore, for agents to employ approaches to minimize the latency they experience in P2P networks. **In this work, we initiate the study of strategic latency reduction in blockchain P2P networks.** We focus on techniques by which agents in such networks can lower the latencies they experience—particularly relative to other agents.

1.1 Types of network latency

In our investigations, we explore two types of latency that play a key role in blockchain P2P networks: *direct latency* and *triangular latency* (formal definitions in §3).

Direct latency refers to the latency with which messages reach a listener node from one or more vantage points—in other words, source latency. We consider two variants:

- *Direct targeted latency* is the delay between a transaction being pushed onto the network by a specific target node (the *victim*) and a node belonging to a given agent receiving the transaction, averaged across all transactions produced by the victim. We can view targeted latency either in terms of an absolute latency, or a relative latency compared to other nodes receiving the same transaction; we focus in this paper on relative latency.
- *Direct global latency* for a given agent’s node refers to targeted latency for that node averaged over all source nodes in the network. In other words, there is no single target victim.

Triangular latency is a second type of latency that corresponds to a node’s ability to inject itself between a pair of communicating nodes. Low triangular latency is motivated by (for example) a node’s desire to front-run another node’s transactions.

We consider two forms of triangular latency:

- *Triangular targeted latency* refers to the ability of an agent’s node v to “shortcut” paths between a sender s (e.g., the creator of a transaction) and a receiver r (e.g., a miner or miners). That is, suppose s creates a transaction m that is meant to reach a (set of) target nodes r . Triangular targeted latency measures the difference between the total delay on path $s \rightarrow v \rightarrow r$ and the smallest delay over all paths from $s \rightarrow r$ not involving v . Given negative triangular targeted latency, an agent can front-run successfully by injecting a competing transaction m' into v upon seeing a victim’s transaction m .
- *Triangular global latency* refers to the triangular relative targeted latency averaged over all source-destination pairs in the network.

It is possible to minimize direct measurement latency without minimizing triangular latency and vice versa. *The two forms of latency are closely related*, however, as we explain in §3 and §6.

1.2 Latency-reduction strategies

High-frequency trading (HFT) firms in the traditional finance industry compete aggressively to reduce the latency of their trading platforms and connections to markets—in some cases, by mere nanoseconds. They invest heavily in technologies that can reduce their communication latency, such as hollow-core fiber optics [36] and satellite links [35].

Such approaches are not a viable means of improving latency over blockchain P2P networks, in which *network topology* matters more than individual nodes’ hardware configurations. These networks are also permissionless, meaning that they experience high rates of churn. Their topology changes frequently and isn’t under the control of any one entity or even any small subset of entities.

Nodes may rely on proprietary, *cut-through* networks to learn transactions and/or blocks quickly. Miners maintain private networks [8]. There are also public, paid cut-through networks. The best known—and a focus of our work—is bloXroute [5].

An agent in a blockchain P2P network, however, can also act strategically by means of *local actions*, namely choosing which peers a node under its control connects to.

Peri: A recently-proposed protocol called Perigee [29] leverages agents’ ability in blockchain P2P networks to control their peering in order to achieve *systemic*, i.e., network-wide, latency improvements. In the Perigee protocol, *every* node favors peers that relay blocks quickly and rejects peers that fail to do so.

A key observation in our work here, however, is that Perigee-like strategies can instead be adopted by *individual strategic agents*. We adopt a set of latency-reduction strategies called **Peri**² that modify Perigee based on this observation and use optimizations that we introduce for the individual-agent setting.

A major question we explore in this paper is whether agents using Peri can gain a latency advantage over other agents, e.g., in the service of strategic goals like the four enumerated above. We show empirically that an agent *can* use Peri to reduce direct and triangular latency, both targeted and global.

1.3 Our contributions

In general, in this work, we explore techniques for an agent to reduce direct measurement latency and triangular latency in a blockchain P2P network using only *local peering choices*, i.e., those of node(s) controlled by the agent. **Overall, we find that strategic latency reduction is possible, both in theory and in practice.** Our contributions are as follows.

- **Practical strategic peering:** We demonstrate empirically and in simulation that the strategic peering scheme Peri can achieve direct latency improvement compared to the current status quo in the Ethereum P2P network.³ We instrument the geth Ethereum client to measure direct measurement latency and implement Peri. We observe direct global latency and direct targeted latency reductions each of about 11 ms—over half the reduction observed for bloXroute for direct latency and comparable to that of bloXroute for targeted latency. Our client modifications incur

²A mischievous winged spirit in Persian lore.

³We explicitly do not consider the design of Peri to be our main contribution, as the design is very similar to Perigee. We make a distinction between the two purely to highlight their differing goals and implementation details.

no extra cost, while bloXroute is a *paid* latency-reduction service. We additionally show in testnet experiments that Peri can discover the IP address of a victim node $7\times$ more frequently than baseline approaches.

- **Hardness of triangular-latency minimization:** We explore the question of strategic triangular-latency reduction via a graph-theoretic model. We show that solving this problem optimally is NP-hard, and the greedy algorithm cannot approximate the global solution. These graph-theoretic results may be of independent interest. We show experimentally in simulations, however, that Peri is effective in reducing such latency.
- **Impossibility of strategy-proof peering protocols:** Within a theoretical model, we prove that *strategy-proof P2P network design is fundamentally unachievable*: For any default peering algorithm used by nodes in a P2P network, as long as the network experiences natural churn and a target node is active, a strategic agent can always reduce direct targeted latency relative to agents following the default peering algorithm. Specifically, with probability at least $1 - \epsilon$ for any $\epsilon \in (0, 1)$, an agent can connect directly to a victim in time $O(\epsilon^{-1} \log^2(\epsilon^{-1}))$.

Overall, our results highlight that it is both feasible and inevitable that agents will reduce their network latency in P2P blockchain networks. Our results have implications for fairness in blockchain applications such as decentralized finance, as they suggest ways that traders may advantage themselves through strategic network positioning. Our results also bear on the security of P2P nodes, as we show how adversarial agents can discover nodes' IP addresses for purposes such as targeted denial-of-service attacks.

2 BACKGROUND AND RELATED WORK

For the sake of concreteness, we focus on the Ethereum network in this work. Many of the latency-sensitive applications discussed in §1 arise in the context of decentralized finance (DeFi) and require a blockchain platform that supports general smart contracts. The general concepts discussed in this work (and the theoretical analysis) apply more broadly to other blockchain P2P networks.

Network Formation. Ethereum, like most permissionless blockchains, maintains a P2P network among its nodes. Each node is represented by its enode ID, which encodes the node's IP address and TCP and UDP ports [42]. Nodes in the network learn about each other via a node discovery protocol based on the Kademlia distributed hash table (DHT) protocol [30]. To bootstrap after a quiescent period or upon first joining the network, a node either queries its previous peers or hard-coded bootstrap peers about other nodes in the network. Specifically, it sends a FINDNODE request using its own enode ID as the DHT query seed. The node's peers respond with the enode IDs and IP addresses of those nodes in their own peer tables that have IDs closest in distance to the query ID. Nodes use these responses to populate their local peer tables and identify new potential peers.

Transaction Propagation. When a user wants to make a transaction, they first cryptographically sign the transaction using a fixed public key, then broadcast the signed transaction over the P2P network using a simple flooding protocol [7]. Each node v , upon

seeing a new transaction m , first checks the validity of the transaction; if the transaction passes basic validity checks, it is added to v 's local TxPool, which consists of unconfirmed transactions. Then, v executes a simple three-step process: (1) It chooses a small random subset $\{u_i\}$ of its connected peer nodes; (2) v sends a transaction hash $H(m)$ to each peer u_i ; (3) If u_i has already seen transaction m , it communicates this to the sender v ; otherwise it responds with a GetTx request, and v in turn sends m in full [42]. There are two main sources of latency in the P2P network: (1) network latency, which stems from sending messages over a P2P overlay of the public Internet, (2) node latency, which stems from local computation at each node before relaying a transaction. In this work, we treat node latency as fixed and try to manipulate network latency.

Transaction Confirmation. After transactions are disseminated over the P2P network, special nodes known as *miners* confirm transactions from the TxPool by compiling them into blocks [33, 42]. The exact confirmation process is not important to our work; the key observation is that when forming blocks, miners choose the order in which transactions will be executed in the final ledger. As discussed in §2.0.1, this ordering can have significant financial repercussions. Miners typically choose the ordering of transactions in a block based on a combination of (a) transactions' time of arrival, and (b) incentives and fees associated with mining a transaction in a particular order. In Ethereum, each block has a base fee, which is the minimum cost for being included in the block. In addition, transaction creators add a tip (priority fee), which is paid to the miner to incentivize inclusion of the transaction in a block [1, 38]. These fees are commonly called *gas fees* in the Ethereum ecosystem.

2.0.1 Example: The role of latency in arbitrage. Among the applications in §1, the interplay between network latency and arbitrage is particularly delicate. To perform successful arbitrage, the arbitrageur must often make a front-running transaction f immediately before the target transaction m , i.e., the transactions f and m are mined within the same block, but f is executed before m . Techniques for achieving this goal have shifted over time.

Before 2020, arbitrage on the Ethereum blockchain happened mostly via priority gas auctions (PGAs), in which arbitrageurs would observe a victim transaction, then publicly broadcast front-running transactions with progressively higher gas prices [15]. The arbitrageur with the highest gas price would win. In this setting, it benefits an arbitrageur to have a low triangular targeted latency (Definition 3.3) between target source nodes (e.g., the victim, other arbitrageurs) and a destination miner, or a low direct targeted latency (Definition 3.1) to a miner. Low latency implies swifter reactions to competing bids on the gas price, and hence more rebidding opportunities before the block is finalized.

In 2020, the mechanisms for arbitrage began to shift to private auction channels like Flashbots [10], in which an arbitrageur submits a miner-extractable-value (MEV) bundle with a tip for miners to a public relay that privately forwards the bundle to miners. A typical bundle consists of a front-running transaction and the target transaction, where the order of transactions is decided by the creator and cannot be changed by the miner of the bundle. Among competing bundles (which conflict with each other by including the same victim transaction), the one with the highest tip is mined.

The key difference from PGA is that an arbitrageur is no longer aware of the tips of its competitors; tips are chosen blindly to balance cost and chance of success. However, the tip is upper-bounded for a rational arbitrageur, because the arbitraging gain is determined by the victim transaction itself. Competing arbitrageurs may set up a grim trigger on the percentage of the tip compared to the arbitrage profit [15]. For instance, they may agree that the tip must not exceed 80% of the profit, so that 20% of profit is guaranteed for the winner. Assuming that every arbitrageur is paying the miner with the same maximum tip, the competition collapses to one of speed. Therefore, even with MEV bundles, network latency remains a critical component of arbitrage success.

2.1 Related Work

Reducing P2P network latency has been a topic of significant interest in the blockchain community. There have been two relevant classes of work for reducing latency: (1) decentralized protocol changes, and (2) centralized relay networks.

Decentralized Protocol Changes. A number of decentralized protocols have been proposed to reduce the latency of propagating blocks and/or transactions. Several of these focus on reducing bandwidth usage, and reap latency benefits as a secondary effect. For example, Erlay [34] uses set reconciliation to reduce bandwidth costs of transaction propagation, and Shrec [21] further designs a new encoding of transactions and a new relay protocol. These approaches are complementary to our results, which are not unique to the broadcast protocol or to the encoding scheme for transactions.

Another body of work has attempted to bypass the effects of latency and peer churn on the topology of the P2P network by creating highly-structured networks and/or propagation paths while maintaining an open network. The Overchain protocol [11] proposes a hypercubic overlay P2P network able to bootstrap new nodes in a decentralized manner while handling high network churn. In [40], the authors compare information dissemination network performance of various network topologies and find that a hypercube performs best in propagation delay and resilience to adversaries. Another protocol, KadCast [37], uses a Kademlia structured overlay network to create routes for block and transaction propagation to reduce complexity and overhead of flooding messages on the network. Such highly-structured networks would be resilient to simple peering-choice strategies like Peri.

Centralized Relay Networks. There have been multiple efforts to build centrally-operated, geographically-distributed relay networks for blockchain transactions and blocks. These include bloXroute [5], Fibre [8], Bitcoin Relay Network [41], and the Falcon network [41]. In this work, we evaluate the latency reduction of centralized services, using bloXroute as a representative example that operates on the Ethereum blockchain. Nodes in the Ethereum P2P network connect to the bloXroute relay network via a gateway, which can either be local or hosted in the cloud [2]. BloXroute offers different tiers of service, which affect the resources available to a subscriber.

3 MODEL

We begin by precisely defining direct and triangular latency, both global and targeted variants. In Table 1, we show the relationship

	<div> ● Target node(s) ● Agent node(s) — Agent-initiated connections </div>	
	Targeted	Global
Direct Latency		
Optimized by	Directly connecting to target (§3.1)	SS-ASPDm approximation algorithm [31]
Triangular Latency		
Optimized by	Directly connecting to targets (§3.2)	Unknown (§6.1)
Main Challenge	Don't know the IP addresses of targets (§7.2.1)	Don't know the graph topology, computational hardness of algorithms (§3.1, §6.1)

Table 1: Summary of challenges and algorithms for optimizing direct and triangular latency, both targeted and global.

between these metrics, and summarize what is currently known (and unknown) about how to optimize them. In this figure, solid red nodes represent a strategic agent. Blue striped nodes represent target nodes in targeted latency metrics. Red thick lines represent the edges (peer connections) that can be formed by the agent to attempt to optimize its network latency.

We model the P2P network \mathcal{N} as a (possibly weighted) graph $(\mathcal{V}, \mathcal{E})$. Let $d_{\mathcal{N}}(s, t)$ denote the shortest distance between s and t over a graph \mathcal{N} . Each individual node $v \in \mathcal{V}$ can create a message m and broadcast it to the network. The message m traverses all the nodes in \mathcal{V} following the network protocol, which allows an arbitrary node to forward the message m upon receipt to a subset of its neighbors.

A participant of the P2P network has two classes of identifiers:

- Class 1. **(Network ID)** An ID assigned uniquely to each of its nodes. For example, each node in the Ethereum P2P network is assigned a unique enode ID including the IP address. For simplicity, we let \mathcal{V} denote the ID space, and a node $v \in \mathcal{V}$ represents an ID instance.
- Class 2. **(Logical ID)** An ID that is used to identify the creator or owner of a message (e.g., the public key of a wallet). We let \mathcal{W} denote the ID space.

In typical blockchain networks, a participant may own multiple instances of both classes. In our analysis, we assume there exists a mapping $f : \mathcal{W} \rightarrow \mathcal{V}$ from a logical ID to a network ID for simplicity. Our strategic agent can identify the signer w of a transaction, but is unaware of the mapping f , and hence cannot peer to the transaction sender $v = f(w)$ until it uncovers v .

We assume the source nodes of network traffic S follow a distribution \mathbb{S} with support \mathcal{V} , i.e., \mathbb{S} specifies a probability distribution over transaction emissions by nodes in \mathcal{V} . We let a random variable $\Lambda(a)$ denote the end-to-end traveling time of a message to a from

a random source $S \sim \mathbb{S}$. Further, we let $\Lambda_v(a)$ denote the random variable $\Lambda(a)|S = v$, representing end-to-end traveling time of a message from a single source v to a .

3.1 Direct Latency Metrics

We define direct targeted latency in Def. 3.1 as the expectation of the single-source message travelling time Λ_v .

Definition 3.1. In a P2P network \mathcal{N} , the **direct targeted latency** of node a with respect to a target node v is defined as:

$$L_v(a) \triangleq \mathbb{E} [\Lambda_v(a)].$$

Reducing direct targeted latency can help with applications such as targeted attacks or front-running a specific set of victim nodes. We define direct global latency as follows.

Definition 3.2. In a P2P network \mathcal{N} , the **direct global latency** of node a is defined as:

$$L(a) \triangleq \mathbb{E} [\Lambda(a)].$$

Note that $L(a) = \mathbb{E}_{S \sim \mathbb{S}} [L_S(a)]$, which means the direct global latency equals the average direct targeted latency weighted by traffic source distribution \mathbb{S} . In the absence of a meaningful source node distribution \mathbb{S} , we let \mathbb{S} be the uniform distribution $\text{Unif}(\mathcal{V})$ over the nodes in \mathcal{V} . Reducing direct global latency can help with applications such as improving block composition for miners, or observing arbitrage opportunities across the network as a whole.

3.1.1 Optimizing Direct Latency. We can consider the problem of latency reduction by an agent as an optimization problem. As a simplification to provide basic insights, we assume the network topology is fixed, and the end-to-end delay of an arbitrary message from source s to destination t is proportional to $d(s, t)$, which denotes the distance between s and t on the network. We also assume the agent has a budget of peer links $k \geq 1$. Then, we aim to solve the following problem to optimize direct targeted latency:

$$\begin{aligned} & \text{minimize} \quad L_v(a) \\ & \text{subject to} \quad |\{y \mid (a, y) \in \mathcal{E}\}| \leq k. \end{aligned} \quad (1)$$

The solution to optimization (1) is trivial under our assumption that $d(s, t) \leq d(s, r) + d(r, t)$ for all $r, s, t \in \mathcal{V}$. The agent only needs to add the target v as a peer in order to achieve the minimum targeted latency, as stated in Table 1. However, achieving this is not necessarily trivial: an agent may not know v 's network address (e.g., IP address), even if v 's logical address is known. We discuss this further in §7.2.

The situation is very different with the optimization problem for global latency reduction, which we formulate as follows. Let w_v denote the probability of v being a target source, i.e., a source of messages of interest to the agent. The optimization problem is:

$$\begin{aligned} & \text{minimize} \quad L(a) = \sum_{v \in \mathcal{V} - \{a\}} w_v d(v, a) \\ & \text{subject to} \quad |\{y \mid (a, y) \in \mathcal{E}\}| \leq k. \end{aligned}$$

This problem is called single-source average shortest path distance minimization (SS-ASPDM) [31]. It is NP-hard, but has an α -approximate algorithm [31].

3.2 Triangular Latency Metrics

Triangular latency is motivated by applications related to front-running in P2P networks. It is defined with respect to one or more pairs of target nodes, where a pair of target nodes includes a source node s and destination node t . For example, consider Table 1 (Triangular Targeted Latency), and let s represent the creator of a transaction and t a miner. The goal of agent node a is to establish a path $s \rightarrow a \rightarrow t$ with lower travel time than any path on \mathcal{N} from s to t excluding a . It can do so by adding edges to the P2P network, which are shown in red in Table 1; note that the (shortest) path from s to a to t is four hops, whereas the shortest path from s to t excluding a is five hops. The existence of such a path enables a to front-run s 's transactions that are mined by t .

We let L'_a denote the direct targeted latency with respect to u on the network excluding the agent a and its incident edges. As a front-runner, a aims to satisfy the following condition:

$$L'_s(t) > L_s(a) + L_t(a). \quad (2)$$

Here we assume the symmetry of targeted latency, i.e., $L_t(a) = L_a(t)$. The left-hand side $L'_s(t)$ is a constant, while the right-hand side depends on the neighbors of a over the P2P network $\mathcal{N} = (\mathcal{V}, \mathcal{E})$; we define this quantity as triangular targeted latency.

Definition 3.3. In a P2P network \mathcal{N} , the **triangular targeted latency** of node a with respect to a target pair (s, t) is defined as

$$L_{s,t}(a) \triangleq L_s(a) + L_t(a).$$

As before, we can optimize this metric subject to a budget constraint on the number of peer connections maintained by the agent:

$$\begin{aligned} & \text{minimize} \quad L_{s,t}(a) \\ & \text{subject to} \quad |\{y \mid (a, y) \in \mathcal{E}\}| \leq k. \end{aligned} \quad (3)$$

The optimal strategy for solving (3) is again trivial: the agent should connect to both s and t (Table 1). Hence, to optimize for a single source and destination, it is key to find s and t on the network and to ensure (2) holds. We discuss this further in §7.

For the rest of the section, we instead consider an agent who attempts to manipulate the *global* triangular latency and capture front-running opportunities over the entire network.

We start with a logical, but ultimately unsatisfactory, definition of triangular global latency. Let Q denote the set of source-destination pairs of network traffic. A front-running agent might naïvely try to optimize the following quantity:

$$L_Q(a) \triangleq \sum_{(s,t) \in Q} L_{s,t}(a) = \sum_{(s,t) \in Q} L_s(a) + L_t(a). \quad (4)$$

This is a variation of the SS-ASPDM problem discussed previously in §3.1. Note, however, that an agent with minimal aggregated pairwise triangular latency L_Q may *not gain maximum profit from front-running*. To gain profit, the agent needs to ensure the inequality (2) holds for pairs (s, t) not necessarily that right-hand side in (4) is minimized.

We thus define the following proxy metric for triangular global latency, which instead measures the quality of peering choices

made by front-runners. Intuitively, the metric counts the number of node pairs (s, t) that an adversarial agent can shortcut, and it is desired to be as high as possible. For example, in Table 1 (Triangular Global Latency), the agent a is allowed to add three edges to the network, and its goal is to select those edges so as to shortcut the maximum number of node pairs (s, t) from network \mathcal{N} .

Definition 3.4. Let $a \notin \mathcal{V}$ denote an adversarial agent node, and $U \subseteq \mathcal{V}$ the set of a 's peers. $\mathcal{N}' = (\mathcal{V}', \mathcal{E}')$ represents the network modified by the agent a , where $\mathcal{V}' = \mathcal{V} \cup \{a\}$ and $\mathcal{E}' = \mathcal{E} \cup \bigcup_{u \in U} (u, a)$. Let $\mathcal{S}, \mathcal{T} \subseteq \mathcal{V}$ be the sets of sources and destinations, respectively. The agent node a has a static distance penalty τ , which means that it can only successfully front-run a source-destination pair (s, t) if the path $s \rightarrow a \rightarrow t$ is at least τ units shorter than the shortest path $s \rightarrow t$ on \mathcal{N} that does not pass through a . The **adversarial advantage** is defined as

$$A_{\mathcal{N}}(U) = \sum_{s \in \mathcal{S}, t \in \mathcal{T}} \left(\mathbb{I}[d_{\mathcal{N}'}(s, t) + \tau < d_{\mathcal{N}}(s, t)] + \frac{1}{2} \cdot \mathbb{I}[d_{\mathcal{N}'}(s, t) + \tau = d_{\mathcal{N}}(s, t)] \right). \quad (5)$$

In practice, \mathcal{T} is the set of miners, and $\tau \in [0, \infty)$ is a parameter that depends on the computational capabilities of the agent, as well as randomness in the network. Ideally, we assume \mathcal{N} is uniformly weighted. We also assume the weights of adversarial links $d_{\mathcal{N}'}(u, a) = 0$ for all $u \in U$, so that we have maximum flexibility in controlling the time costs over these links with parameter τ .

3.3 Summary

In summary, existing latency metrics are informative as they express natural strategic-agent goals. They are difficult to optimize directly, however, due to a combination of strong knowledge requirements about the P2P network, high computational complexity, and/or assumptions about the stationarity of the underlying network. For example, to optimize global latency, we require two key assumptions that are unrealistic for P2P networks: the network topology should be static and the agent should know both the network topology and traffic patterns. To optimize targeted latency, we require knowledge of the target node's network ID, i.e., its IP address; this is often unknown in practice. These challenges motivate the Peri algorithm in §4, which avoids all the above assumptions.

4 DESIGN

As we saw in §3, optimizing network latency requires knowledge of the network topology and/or node network addresses, which are unknown for typical P2P networks. Instead, an agent is typically only aware of its own peers, i.e., its neighbors in the network. In this section, we present the Peri peering algorithm to account for this observation, and achieve *reduced* (if not necessarily optimal) latency. Peri is a variant of the Perigee [29] algorithm, which was initially proposed as a network-wide technique for reducing transaction broadcast latency.

4.1 Perigee

Perigee was introduced in [29] as a decentralized algorithm for generating network topologies with reduced broadcast latency for

transactions and blocks. The Perigee algorithm is presented in Alg. 1. Lines that are highlighted in **red** are specific to Peri (§4.2).

Input: Number of peers K kept after each iteration, maximum peer count N , length of period T , score function ϕ

Result: Peer set P at each period $h = 1, 2, \dots$

```

1  $P \leftarrow \emptyset, B \leftarrow \emptyset;$  //  $B$  is a blocklist of evicted peers
2 Run Thread peer_manager():
3   while true do
4     Hang and wait for next peer;
5      $v \leftarrow$  Random sampled node from  $\mathcal{V} - B$ ;
6     if  $|P| < N$  then
7        $P \leftarrow P \cup \{v\};$  // add peer when a slot is available
8   for  $h \leftarrow 1, 2, \dots$  do
9     Sleep  $T$ ; // peer_manager adds peers to  $P$  when sleeping
10     $e \leftarrow N - K;$  //  $e$  is the number of peers to evict
11    Init score map  $\Phi$ ;
12    for  $p \in P$  do
13      if not is_excused( $p$ ) then
14         $\Phi(p) \leftarrow \phi(p);$ 
15      else
16         $e \leftarrow e - 1;$ 
17    if  $e > 0$  then
18       $P \leftarrow P - \text{largest\_n\_elements}(\Phi, e);$ 
19       $B \leftarrow B \cup \text{largest\_n\_elements}(\Phi, e);$ 
20    Output  $(h, P);$ 

```

Algorithm 1: Perigee [29]/ Peri. Red text denotes parts that are specific to Peri. Note: `is_excused` is a predicate that is true when peer-delay information is insufficient to make a peering decision. $\phi(v)$ equals the average transaction-delivery delay of v with respect to the best peer, as defined in Eqn. (6). It incorporates design choices highlighted in §4.2.

At a high level, Perigee requires every node in the network to assign each of its peers a latency score and periodically tears down connections to peers with high scores. In our context, the latency score represents the latency with which transactions are delivered; we want this score to be as low as possible. Over time, Perigee causes nodes to remain connected to low-latency peers, while replacing other peers with random new ones. Roughly speaking, [29] shows that Perigee converges to a topology that is close to the optimal one, in the sense of minimizing global broadcast latency.

More precisely, Perigee divides time into periods. Let u denote a given node in the network and M_u denote the set of all transactions received by u in the current period from a current peer v . For a given transaction m , let $T(m)$ denote the time when m is first received by u from any of its peers and $T_v(m)$ denote the time when m is received by u specifically from v . We define $T_v(m) = \infty$ if v did not deliver m during the current period.

In every period, each node u evaluates a score function ϕ over each of its peers v , defined as

$$\phi(v) \triangleq \sum_{m \in M_v} \frac{1}{|M_v|} \min \{T_v(m) - T(m), \bar{\Delta}\}. \quad (6)$$

Here, $\bar{\Delta}$ is a parameter used by Perigee as an upper bound on measured latency differences. Its effect is to bound the influence of outliers on score-function computation.

For a node u , the score function $\phi(v)$ may be viewed as capturing the average over all transactions m of the difference in latency between delivery of m by v and that by the peer from which u first received m . In other words, $\phi(v)$ may be viewed as the average slowdown imposed by v with respect to the fastest delivery of transactions to u .

We briefly explain one element of the algorithm: the procedure `peer_manager` is an asynchronous thread (or set of threads) that handles peer connections on the P2P network, including accepting incoming peer requests, requesting nodes for connection and dropping peers. Ideally, it can randomly sample nodes from the entire network, gradually add peers when the peer count is under the maximum, and keep connections with specific nodes (targets). Hence, while the main thread sleeps, `peer_manager` expands the peer set P until it reaches its maximum size N .

4.2 Peri

Although Perigee was designed to be deployed by *all* network nodes to improve broadcast latency, we observe that the same ideas can be applied by a single agent to improve their observed direct and triangular latency. In this section, we describe Peri, which is a slight modification of Perigee enabling an agent to control their direct and triangular latency. Although Peri does not differ from Perigee in its basic approach, we give them different names to differentiate their usage and certain key implementation choices. Again, the steps unique to Peri are highlighted in **Red** in Alg. 1. Peri will be a key baseline for all of our experiments in §5 and §6.

The main differences between Perigee and Peri are:

- (a) **Goal:** Peri is meant to be applied by a single node to advantage it over other nodes, whereas Perigee was proposed as a protocol to optimize systemic network performance.
- (b) **Relevant transactions:** In Perigee, nodes measure the latency of all received transactions. In Peri, the score function $\phi(v)$ enforces that only *relevant transactions* participate in scoring peers. In Peri, for direct global latency reduction, all transactions are considered relevant, while for direct targeted latency reduction, only transactions made by the target are relevant.
- (c) **Handling silent peers:** Particularly when optimizing targeted latency, the function ϕ may be undefined for some peers in some periods. For example, if a peer p is connected near the end of a given period, there will not be sufficient data to compare p with other peers, which means $\phi(p)$ may be undefined. Instead of evicting p in such cases and possibly losing a good peer, we forego eviction of p . In Alg. 1, the predicate `is_excused(v)` is true if node v should be excluded from eviction for the current period.
- (d) **Blocklists.** The Perigee [29] algorithm advocates for selecting a new set of peers at random. However, this increases the likelihood of a peer tearing down connections, then connecting to the same node(s) shortly thereafter, particularly since some cryptocurrency clients (including `geth`) favor previously-visited nodes during peer selection [22, 23]. To handle this, in Peri we use *blocklists*: if a node tears down a connection to peer v in a Peri period, it refuses to re-connect to v in future periods. In Alg. 1, we maintain blocklist B for this purpose.
- (e) **Sampling relevant transactions:** Note that we cannot relay relevant transactions; otherwise, the “late” peers who do not deliver a relevant transaction first to our node will *never* deliver it to our node (§2), thus removing them from Peri’s latency comparison. If all transactions are treated as relevant, our node will act as a black hole for transactions, and may impact the P2P network. We avoid this issue by sampling 1/4 of all (relevant) transactions for global latency measurement. This is realized by redefining relevant transactions as those with hashes divisible by 4 when computing $\phi(\cdot)$ in Line 14 of Algorithm 1.

5 DIRECT LATENCY EVALUATION

In §5.1 and §5.2, we show the practical latency reduction effects of Peri with experiments on the Ethereum P2P main network (mainnet) and Rinkeby test network (testnet).

5.1 Evaluation: Direct Global Latency

We start by evaluating the feasibility of reducing global latency.

5.1.1 Methods. We evaluate four approaches.

- (a) **Baseline.** Our experimental control node uses the default settings of the Go-Ethereum client, version 1.10.16-unstable [9]⁴. This was the latest version when we started the experiments.
- (b) **BloXroute.** We compare against a centralized, private relay network, using bloXroute as a representative example. We use the bloXroute Professional Plan [5]; at the time our experiments were run, this plan cost \$300 per month. We ran the bloXroute gateway locally to avoid incurring additional latency (§2.1).
- (c) **Peri.** We modify the Go-Ethereum client [9] to implement the Peri algorithm for peer selection. We set the period to 20 minutes, and replace at most 25 peers every period.
- (d) **Hybrid.** We implement a hybrid method that combines bloXroute and Peri by applying Peri to a node with access to a bloXroute relay. To ensure correctness, we ensure that the gateway connecting to the relay, which acts as a peer of the node, cannot be removed by the Peri algorithm.

5.1.2 Experimental Setup. We establish 4 EC2 instances in the us-east-1 AWS data center, where a public bloXroute relay is located. On each instance, we deploy a full node on the Ethereum P2P main network (the mainnet), which is implemented by a customized Go-Ethereum (`geth`) client. Each node has at most 50 peers, which is the default setting of Go-Ethereum. For a node running Peri or Hybrid, we set the proportion of outbound peers (peers dialed by the node itself) to 80% so that the node actively searches for new peers. For a node running other baselines, we keep the proportion at 33%, which is also default for Go-Ethereum.

We ran 63 experiments from Feb 18, 2022 to March 16, 2022, each following the procedure below. First, we assign each latency reduction method (bloXroute, Peri, Hybrid and Baseline) exclusively to a single node, so that all four nodes use different comparison methods. Then, we launch the nodes simultaneously. When a packet arrives, the node checks if the packet contains a full relevant transaction or its hash; if so, it records the timestamp. At the end of the

⁴The customized client source code can be found at https://github.com/WeizhaoT/geth_peri.

experiment, we stop the nodes and collect the arrival timestamps of transactions from their host instances.

Bias reduction. We take the following steps to control for systematic bias in our experiments. We prohibit the 4 measurement nodes from adding each other as peers. We reset all the enode IDs (unique identifiers of the Ethereum nodes including IP address) before each experiment. This prevents the other nodes from remembering our nodes’ IP addresses and making peering decisions based on activity from previous experiments. We record the clock differences with periodic NTP queries between each pair of hosts to fix systematic errors in the timestamps recorded locally by the hosts. Despite being the same type of AWS instance, the host machines may also introduce biases because they may provide different runtime environments for the Ethereum node program. To eliminate these biases, we rotate the assignment of latency reduction methods after every experiment, so that for every successive 4 experiments, each node is assigned each method exactly once. We attempt to control for temporal biases due to diurnal transaction traffic patterns by running each experiment every 8 hours, so that the assignment of methods to nodes rotates 3 times a day. Because the number of possible method assignments is 4, a co-prime of 3, each node experiences every combination of latency reduction methods and time-of-day. We did not control for contention (e.g., of network bandwidth, computational resources) among EC2 instances by running experiments on dedicated hardware due to financial constraints.

5.1.3 Results. Each node is allowed to warm up for 2.5 hours; after this, we collect all transactions that are received by each of the nodes for 3.5 hours. Then, for each transaction m and each node y with a latency reduction method other than Baseline, we compute the difference between the timestamp of m at y and the timestamp at the baseline node b , which is effectively a sample of random variable $\Lambda(y) - \Lambda(b)$. The smaller the time difference (i.e., the more negative), the earlier y delivers m , and the more effective the latency reduction method is. We gather the latency differences over 63 experiments, and plot their distributions for each node in Fig. 1. In total, we analyzed the latencies of 6,228,520 transactions.

Finding 1: Peri alone is at least half as effective as bloXroute private networks in reducing average direct global latency. The Hybrid node (combining Peri with bloXroute) is superior to bloXroute, achieving an additional 15% improvement in latency reduction over bloXroute alone.

In the figure, all the latency differences are distributed with negative means and medians, showing an effective latency reduction. To establish the statistical significance of the mean difference among these distributions, we first perform the Kruskal-Wallis H test [25]. The resulting p-value equals 0, so that a following Dunn’s test is recommended. We perform Dunn’s test [18] with the Bonferroni correction [13], and obtained a 0 p-value between each pair of distributions. This test supports statistically significant differences in the reduction of direct global latency effected by the three methods, ordered by the means of their corresponding distributions. BloXroute reduced this latency by 18.45 milliseconds on average. In comparison, Peri reduced it by 11.09 milliseconds, which is more than half as effective as bloXroute, and at the same time *cost-free*,

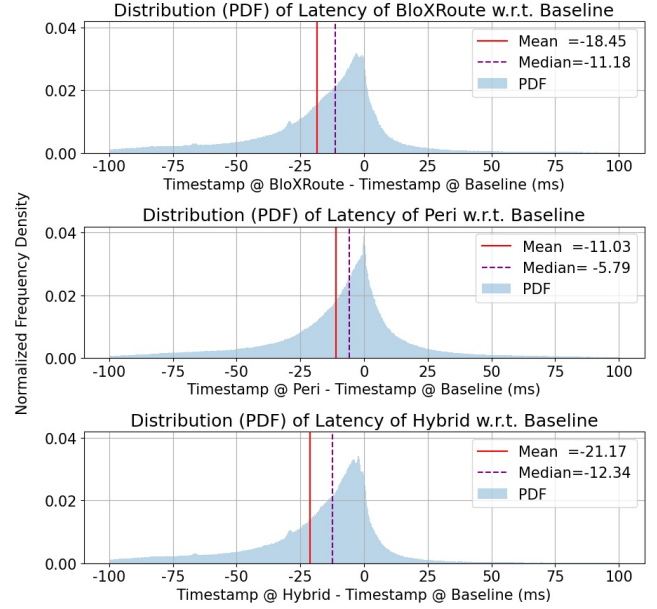


Figure 1: PDFs of distributions of global latency.

in the sense that it does not require payment of the \$300 / month of the bloXroute plan used in our experiments. On the other hand, by exploiting access to bloXroute services, Hybrid nodes can achieve an *additional* 15% reduction in latency. This suggests the potential of peer-selection algorithms to further boost latency reduction techniques over purely private relay networks.

5.2 Evaluation: Direct Targeted Latency

Reducing direct targeted latency is useful for different applications compared to reducing direct global latency. An agent with a low direct targeted latency can perform better targeted arbitraging against a specific victim, or discover the IP address of a target cryptocurrency node. In this section, we evaluate the feasibility of reducing direct targeted latency. We apply the same methods we used to reduce direct global latency.

Experimentally evaluating targeted latency reduction techniques on the Ethereum mainnet can be costly and time-consuming. This is because to evaluate latency distributions, we need to observe many transactions with a known ground truth IP address. A natural approach is to generate our own transactions from a single node and measure their latency; unfortunately, nodes in the P2P network do not forward transactions that are invalid or unlikely to be mined due to low gas fees. Hence, we would need to create valid transactions. For example, at the time of writing this paper, the recommended base fee of a single transaction was about \$2.36 per transaction [6]. Collecting even a fraction of the 6+ million transactions analyzed in §5.1 would quickly become prohibitively costly.

We ran limited experiments on direct targeted latency, where the setups and results are shown in details in Appendix A.2. The findings of these experiments are summarized below.

Finding 2: Peri reduces direct targeted latency by 14% of the end-to-end delay, which is as effective as bloXroute and Hybrid.

Unfortunately, we did not collect a sufficient amount of data for Peri and Hybrid to show a statistically significant ability to connect directly to a victim and learn its IP address. We attribute this to the low transaction frequency and large size of the mainnet. The testnet experiments we now describe, however, *did* result in frequent victim discovery of this kind—provided a sufficiently large number of Peri periods or a high frequency of victim transactions.

5.2.1 Targeted Latency on Ethereum testnets. Due to the financial cost of latency reduction experiments at scale on the Ethereum mainnet, we also performed experiments on the Rinkeby testnet.⁵ Our goal in these experiments is to simulate a highly active victim in the network and compare the Peri algorithm’s ability to find and connect to the victim against a baseline default client.

In these experiments we run a victim client on an EC2 instance in the ap-northeast-1 location and the Peri and Baseline clients in the us-east-2 location. Note that we cannot evaluate bloXroute or Hybrid on the test network, because bloXroute does not support test network traffic. Due to our observations of the Rinkeby network’s smaller size, and to emulate a long-running victim whose peer slots are frequently full, we set the peer cap of the victim to 25 peers. As in previous experiments, the Baseline node is running the default geth client with peer cap of 50. The Peri node is also running with a peer cap of 50 but with the Peri period shortened to 2 minutes.

In each experiment, we start the victim client first and give it a 30 minute warm-up period to ensure its peer slots are filled. We then start the Peri and Baseline nodes and begin transmitting transactions from multiple accounts on the victim node. We set the frequency to 3 transactions per minute to control the variance of timestamps and Peri scores. We then run the experiment for just under 3 hours, enabling us to run 7 experiments per day and alleviate time-of-day biases. As with the global latency experiments in §5.1, we alternate which us-east-2 machine is running Peri v.s. Baseline across runs in order to mitigate potential machine-specific biases. We ran these experiments from April 16th - 26th, 2022, for a total of 70 runs.

Finding 3: In testnet experiments, Peri is able to identify the IP address and connect to a target (victim) node with a frequency more than 7× that of a Baseline node.

The number of connections established by the Peri and Baseline clients to our victim are listed in Table 2. We find that Peri gives a notable advantage in terms of connecting to the victim node. Fig. 2 shows a CDF of the number of Peri periods until Peri connected to the victim, with an mean/median of 39/45 periods (~ 1.3/1.5 hrs). Fig. 3 shows the delay PDF for the runs when Peri finds the victim for all transactions before and after Peri connects to the victim. We observe a mean latency advantage of 22ms over the Baseline client once Peri connects to the victim. This is 30% of the end-to-end

⁵Though the Ropsten testnet is generally thought to be the test network that most faithfully emulates the Ethereum mainnet [3], its behavior was too erratic for our experiments during our period of study. This included high variance in our ability to connect to peers from any machine and constant deep chain reorganizations, causing lags in client synchronization.

Method	Peri	Baseline
Successful Victim Connections	47/70 = 67.1%	6/70 = 8.6%

Table 2: Rate of connection to victim node in Rinkeby test-net experiments.

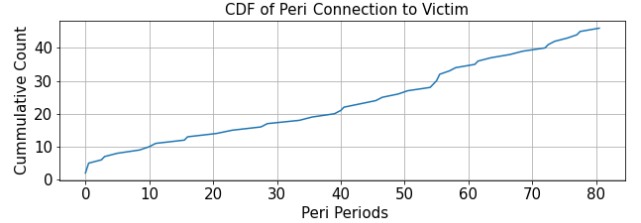


Figure 2: CDF of number of Peri periods before finding victim. Each Peri period lasts 2 minutes.

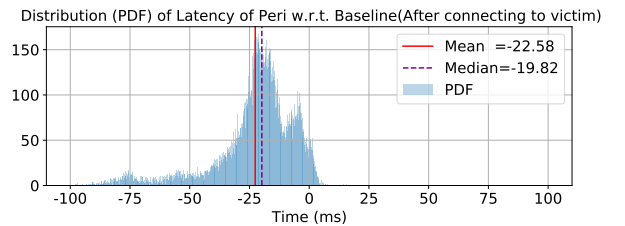
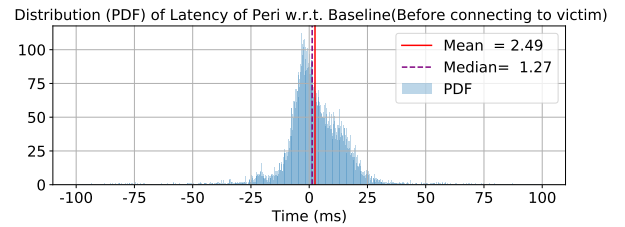


Figure 3: PDFs of distributions of targeted latency for runs when Peri found the victim split between before either found the victim, and after Peri finds the victim. The x axis represents the difference of timestamp at the Peri node and at the baseline node for each single transaction.

delay between the victim and both the Peri and Baseline clients. Unlike the case with our mainnet experiments, though, Peri has no significant advantage before it connects to the victim. We attribute the difficulty of establishing a network advantage prior to direct connection to the victim to the Rinkeby network’s smaller size (1.8K unique IPs we came across over the period of our study compared to 13.6K in the mainnet). A consequence is that there are relatively few peers in geographical proximity to the Tokyo data center by comparison with our mainnet victim node in Germany. There are significant differences in size and topology between the Rinkeby network and the Ethereum mainnet, and it is unclear how our experiments would extrapolate to the mainnet. Our experiments do, however, provide evidence that Peri can boost the likelihood of a strategic agent connecting directly to a victim in P2P networks; how this capability generalizes warrants further investigation.

6 TRIANGULAR LATENCY EVALUATION

As explained in §3, a front-runner may be interested in two types of triangular latency: targeted and global. As with direct targeted latency, we established in §3.2 that the optimal strategy for an agent to reduce triangular targeted latency is to connect directly to the target nodes. Since this procedure is identical to the experiments in §5.2, we do not run additional experiments to demonstrate its feasibility in this section.

The more complicated question is how to optimize triangular global latency. Recall from §3.2 that we study triangular global latency via a proxy metric, which we call *adversarial advantage* $A_N(U)$, where N denotes the network and U denotes the set of strategic or adversarial agents. In the remainder of the section, we first show that directly optimizing adversarial advantage is computationally infeasible even if the agent knows the entire network topology (§6.1). However, we also show through simulation that efficient local strategies (namely, a variant of Peri) can be used to outperform baselines (§6.2).

Note on evaluation: Adversarial advantage is even more difficult to evaluate empirically than direct latency. To measure adversarial advantage for a single source-destination pair, we would need to observe transactions from a known source (e.g., a front-running victim), which end up at a known target destination (e.g., a miner or an auction platform [10]); we would additionally need to verify that our agent node is able to reach the target node *before* the victim’s transaction reaches the target destination. Setting up our own nodes on the mainnet to measure this would be twice as costly as evaluating direct targeted latency (since we would need to generate both a valid victim *and* front-running transaction), which we deemed infeasible in §5.2. Measuring adversarial advantage globally would require visibility into every pair of nodes in the network, which is clearly infeasible. *For these reasons, we chose to evaluate triangular latency reduction theoretically and in simulation.*

6.1 Hardness of Optimizing Adversarial Advantage

Generally, we are interested in the following problem.

PROBLEM 1. *Given a network N , sets of sources and destinations S, \mathcal{T} , and budget k (number of edges the agent can add), we want to maximize $A_N(U)$ (Definition 3.4) subject to $|U| \leq k$, where U is the set of peers to which the agent node connects.*

THEOREM 6.1. *Problem 1 is NP-hard.*

(Proof in Appendix A.1.1) The proof follows from a reduction from the set cover problem. Not only is solving this problem optimally NP-hard, we next show that it is not possible to *approximate* the optimal solution with a greedy algorithm. A natural greedy algorithm that solves the advantage maximization problem is presented in Algorithm 2. (Note that it includes a “bootstrapping” step in which two nodes are initially added to the set U of agent peers, as no advantage is obtainable without at least two such nodes.) The greedy algorithm is *unable* to approximately solve the advantage maximization problem.

PROPOSITION 6.2. *The output of Alg. 2 is not an α -approximate solution to Problem 1 for any $\alpha > 0$.*

Input: Number of peers $k \geq 2$, graph N

Output: Set of peers U

```

1  $U \leftarrow \operatorname{argmax}_{(x,y): (x,y) \in V^2} A_N(\{x, y\});$ 
2 for  $j \in \{3, 4, \dots, k\}$  do
3    $\bar{z} \leftarrow \operatorname{argmax}_{z: z \in V-U} A_N(U \cup \{z\});$ 
4    $U \leftarrow U \cup \{\bar{z}\};$ 
5 return  $U;$ 
```

Algorithm 2: Greedy Algorithm for Maximizing A_N .

(Proof in Appendix A.1.2) We show this by constructing a counterexample for which the greedy algorithm achieves an adversarial advantage whose suboptimality gap grows arbitrarily close to 1 as the problem scales up. Whether a polynomial-time approximation algorithm exists for maximization of A_N is an open problem.

6.2 Approximations of Advantage Maximization

The greedy algorithm in Algorithm 2 is provably suboptimal for maximizing adversarial advantage in general, but we observed in simulation that for small, random network topologies (up to 20 nodes), it attains a near-optimal adversarial advantage (results omitted for space). We also show in this section that the greedy strategy achieves a much higher advantage (2-4 \times) than a natural baseline approach of randomly adding edges. Hence, the greedy strategy may perform well in practice. However, the greedy strategy has a critical flaw: *it requires knowledge of the entire network topology.*

In this section, we evaluate the feasibility of using local methods (i.e., Peri) to approach the performance of the greedy strategy. Because the greedy strategy is centralized, we expect it to outperform Peri. However, we show in simulation⁶ that for several natural graph topologies, this margin is small.

Graph topology. We consider four models of random graph topologies: Erdős-Rényi, random regular graphs, Barabási-Albert (scale free) graphs, and Watts-Strogatz (small world) graphs. The Ethereum P2P network has been shown to exhibit properties of both small world and scale-free networks [42]. The number of nodes is set to 300 for all the models. The average degree is set to 9 for the Erdős-Rényi model to ensure connectivity. The average degree, however, is set to 4 for the other 3 models to make sure the average distance between nodes is high enough for shortcuts to exist. For each model, we sample 25 different graph instances. Further, we centralize each instance by introducing 20 new hub nodes, each connecting to 30 nodes randomly sampled from the original graph.

On each instance, the set of sources S is equal to the set of all the nodes V , and the set of destinations \mathcal{T} is a random subset of V with $|\mathcal{T}| = 0.1 \cdot |V|$. We let the static front-running penalty $\tau = 0$, a minimum path advantage, and assign a unit weight to all the edges.

Peri Modification. To make Peri optimize adversarial advantage, we alter the scoring function and the peer-selection criterion. This alteration in turn reveals a clean way of simulating the (modified) Peri algorithm without simulating individual message transmissions. First, we make the following simplifying assumptions: (a)

⁶The simulator code can be found at <https://github.com/WeizhaoT/Triangular-Latency-Simulator>.

Peer replacement is completed immediately at the beginning of a new Peri period, and no peer is added or dropped during the period; (b) The full set M of messages sent during the current Peri period is delivered to the adversarial agent during the Peri period by every peer; (c) The end-to-end delay of each message is proportional to the distance between its source and destination; and (d) Message origination is uniformly distributed over the network.

Let $d_v(m)$ denote the distance from the source of m to peer v of the agent node a and $S(m)$ the time when message m departs from the source. Recall that we assume $d_{\mathcal{N}'}(v, a) = 0$ for any peer v of a in §3.2, so for such a v , $d_v(m)$ equals the distance from the source of m to a . The score function $\phi(v)$ for peer v can be transformed as follows with constants C_1, C_2, C_3 with respect to v for a set topology.

$$\begin{aligned}\phi(v) &= \sum_{m \in M} \frac{T_v(m) - T(m)}{|M|} = \sum_{m \in M} \frac{T_v(m) - S(m)}{|M|} + \frac{S(m) - T(m)}{|M|} \\ &= C_1 \sum_{m \in M} d_v(m) + C_2 = C_3 \sum_{s \in S} d_{\mathcal{N}'}(s, v) + C_2.\end{aligned}$$

Since Peri’s choice of which peers to drop is invariant to C_2 or C_3 , we can further simplify the score in (7):

$$\phi(v) = \sum_{s \in S} d_{\mathcal{N}'}(s, v). \quad (7)$$

For a given peer budget k , we replace $r = \left\lceil \frac{k}{3} \right\rceil$ peers and keep k peers. We only consider the kept peers for evaluation of the advantage metric. In total we execute 800 Peri periods.

Results. We sweep the peer count budget $|U| = k$ of the agent over 7 values ranging from 2 to 20. For each maximum peer count, we obtain a resulting peer set U^* with advantage $A_{\mathcal{N}}(U^*)$ using the greedy algorithm, the Peri algorithm, and random sampling, in which each agent chooses to peer with nodes selected uniformly at random. The performance of each method is represented by its advantage-peer-count ($A_{\mathcal{N}}(|U|)$) curve. For each graph model, we plot the mean and standard deviation of the curves over 25 different hub-enriched graph instances in Fig. 4.

Finding 4: Peri is competitive with the greedy algorithm for maximizing adversarial advantage when the underlying network has many hubs, or nodes of high degree.

The introduction of hubs is motivated by the simulations of the original topologies without hub nodes, which we show in Appendix A.3. Regardless of the original topology, the existence of hub nodes enables the Peri algorithm to place shortcuts almost as effectively as the greedy algorithm. We notice that Peri worked significantly better on models with more hubs such as scale-free than the other topologies. It is also notable that over 70% of the resulting peers of the Peri algorithm are hubs, which signals the ability of the Peri algorithm to locate hubs and perform front-running attacks through them. Hubs have been shown to be common in real-world cryptocurrency P2P networks [32, 42], motivating Peri to be a potentially powerful tool in practice.

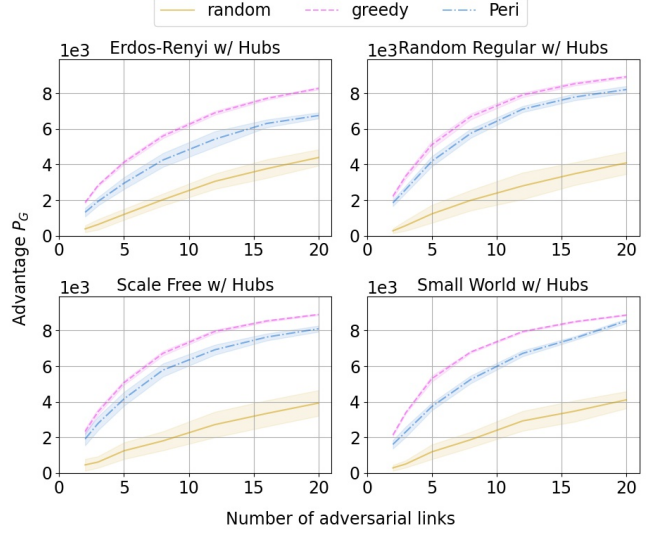


Figure 4: Advantage-Peer-count curves on hub-enriched graph models. The mean of the curves are shown by solid lines, and the standard deviations are shown by the transparent color zones centered at the mean.

7 IMPOSSIBILITY OF STRATEGY-PROOF PEERING PROTOCOLS

We have so far seen that Peri (and variants including the Hybrid approach) can significantly improve direct and triangular latency. A natural question is whether this is because most nodes are currently running a poor peer selection strategy (Baseline). For example, if every node were running Peri or Hybrid, would it still be possible for an agent to strategically improve their targeted latency? we show that no matter what peering strategy nodes are using, as long as the P2P network has some natural churn and as long as the target node(s) are active, a strategic agent can *always* manipulate their targeted latency.

7.1 Model

We start with some additional modeling assumptions regarding the temporal dynamics of our network. Consider a time-varying network $\mathcal{N}(t) = (\mathcal{V}(t), \mathcal{E}(t))$ where $\mathcal{V}(t)$ denotes the set of nodes and $\mathcal{E}(t)$ denotes the set of undirected edges of G at time t . In the network, any party can spawn a set V' of nodes and add them to $\mathcal{V}(t)$. ($\mathcal{V}(t^+) = \mathcal{V}(t) \cup V'$, where t^+ denotes the time infinitesimally after t). We assume there is an upper bound \bar{V} on the total number of nodes in the network; that is, $|\mathcal{V}(t)| \leq \bar{V}$ for all $t \geq 0$, due to the limited address space for nodes.

If a node u knows the network (Class 1) ID of another node v , u can attempt to add an edge, or a peer connection, (u, v) at time t (that is, $\mathcal{E}(t^+) = \mathcal{E}(t) \cup \{(u, v)\}$) to the network. This peering attempt will succeed unless all of v ’s peer connections are full. Nodes have an upper bound of h on their total number of peer connections:

$$\deg(u) \leq h \quad \forall u \in \mathcal{V}(t), \quad \forall t \geq 0.$$

Among these, each node has at least $f \in (0, h]$ **dynamic peer slots**. A connection from u to v that occupies one of either u 's or v 's dynamic peer slots is called *dynamic* and will be periodically torn down (more on this in Definition 7.1). Additionally, a dynamic peer slot is permissionless and is filled first-come-first-serve (FCFS).

We assume there exists an oracle in the network serving as an abstraction of a distributed database of network IDs. Any node may query the oracle, which responds by independently drawing the network ID of a node in the network from some (unknown) probability distribution, where each node may be drawn with a non-zero probability. Specifically, there exists a universal constant $q > 0$ where the probability of drawing an arbitrary node is lower-bounded by q . This is based on the assumption that the number of nodes is upper bounded. We assume the oracle can process a fixed number of queries per unit time, so each query (across all nodes) takes constant time. Upon processing a query, the oracle responds with the network ID of an existing node. This is an abstraction of peer discovery in many blockchains [43].

Each edge $(u, v) \in \mathcal{E}(t)$ has an associated *link distance* $w(u, v)$, which operationally represents the Internet latency from u to v . We assume latency $w(u, v)$ is dominated by the physical length of the path $u \rightarrow v$ on the Internet. Hence, we assume $w(u, v)$ is a constant over time and satisfies the triangle inequality:

$$w(u, v) \leq w(u, z) + w(v, z), \quad \forall u, v, z \in \mathcal{V}(t), t \geq 0. \quad (8)$$

This is distinct from graph distance $d_N(u, v)$ introduced in §3.

Transaction dissemination. A node can broadcast an arbitrary message (transaction) at an arbitrary time through the entire network. When a message is sent from u to its neighbor v at time t , v will receive the message at time $t + w(u, v)$, where $w(u, v)$ is the link distance between u and v . If v is not adversarial, it will immediately forward the message to each of its neighbors.⁷ We assume the P2P network is connected at all times $t \geq 0$. We additionally assume that the latency between any pair of agent nodes is negligible, such that an agent connecting to multiple targets from multiple agent nodes, is equivalent to these targets peering with one node.

Liveness. In our analysis, we will assume that nodes are sufficiently active in terms of producing transactions and that the network experiences some amount of peer churn. We make both of these assumptions precise with the following definition.

Definition 7.1. A (λ, ν) -live network has the following properties:

- (I) All dynamic connections have a random duration $\text{Exp}(\lambda)$.
- (II) For each node $u \in \mathcal{S}$, where \mathcal{S} denotes a set of target nodes, we let $\{M_u(t), t \in [0, \infty)\}$ denote the counting process of messages that are generated and broadcast by u . $M_u(t)$ is a Poisson process with rate ν .

7.2 Optimization of Targeted Latencies

7.2.1 Inferring Network ID. We argue in §3 that we can optimize targeted latency (both direct and triangular) by connecting directly to the target node(s). However, in practice, an agent typically only knows the targets' logical (Class 2) IDs (e.g., public key of wallet), whereas it needs their network (Class 1) IDs (e.g., IP address) to connect. In the following, we show when an adversarial agent can

learn the network ID(s) of one or more targets. Our first result states that in a live network (Definition 7.1), it is possible for an agent to uncover the network ID(s) of a set of target nodes with probability $1 - \varepsilon$ given only their logical IDs in time quasilinear in ε^{-1} and quadratic in the number of target nodes.

THEOREM 7.2. *Consider a live network $N(t) = (\mathcal{V}(t), \mathcal{E}(t))$. Let \mathcal{A} denote an adversarial agent capable of identifying the logical ID of the sender of any message it received from the network. Given a set of target nodes U , with probability at least $1 - \varepsilon$ for any $\varepsilon \in (0, 1)$, it takes the agent $O(|U|^2 \varepsilon^{-1} \log^2 \varepsilon^{-1})$ time to find the network ID of any message sender in $N(t)$.*

(Proof in Appendix A.1.3) The proof shows that a variant of Peri achieves the upper bound, showing Peri's effectiveness. In particular, note that to optimize triangular targeted latency, for a target pair of nodes (s, t) , the agent must connect to both s and t , so $|U| = 2$ in Theorem 7.2.

Additionally, the following proposition shows that regardless of the agent's algorithm, we require time at least logarithmic in $1/\varepsilon$.

PROPOSITION 7.3 (LOWER BOUND). *Consider a live network $N(t) = (\mathcal{V}(t), \mathcal{E}(t))$. Let \mathcal{A} denote an adversary defined in Theorem 7.2. For any $\varepsilon \in (0, 1)$, to achieve a probability at least $1 - \varepsilon$ that the agent is connected to its target, \mathcal{A} must spend at least $\Omega(\log \varepsilon^{-1})$ time, regardless of the algorithm it uses.*

(Proof in Appendix A.1.4) Proposition 7.3 suggests that a node aiming to prevent agents from learning its network ID with probability at least $1 - \varepsilon$, should cycle its logical ID on a timescale of order $\log \varepsilon^{-1}$.

Together, Theorem 7.2 and Proposition 7.3 show how and when an agent can find a message source in a P2P network. They are an important missing piece in the solution to optimization problems (1) and (3) for targeted latency. Next, we discuss how the other missing piece is filled in, i.e., how the agent ensures successful and eternal peer connections with targets after finding them.

7.2.2 Connecting to Targets. By assumption, the target must have at least $f > 0$ dynamic peer slots, which are permissionless and thus can be accessed by the agent. Since these slots are on a FCFS basis, the agent may request an occupied peer slot at an arbitrarily high frequency, such that it immediately gets it when the slot becomes available after the old connection is torn down.⁸ In this way, an agent can effectively make a dynamic peer slot of any target *no longer dynamic*, and constantly dedicated to itself.

7.2.3 Latency Manipulation. Even if the agent is connected to the target, the latency between them is still lower-bounded due to the physical distance between the agent and the target. Agents may be able to relocate their nodes geographically to manipulate triangular latency. Currently, over 25% of Ethereum nodes are running on AWS [4]. An agent can map their IP addresses (§7.2) to the locations of their cloud data centers, and deploy nodes on cloud servers at the same locations. This can reduce the direct targeted latency to the level of microseconds. For triangular targeted latency where the source and the destination are at different geolocations, the agent can deploy node a_1 near the source s and node a_2 near

⁷This is a special case of randomized flooding protocols like diffusion [19].

⁸To evade detection by the frequency of requests from single nodes, an agent can spawn many nodes and split the periodic requests among its nodes.

the destination t , where a_1 connects to s and a_2 connects to t , with a_1 and a_2 connected via a low-latency link. This ensures the path $s \rightarrow a_1 \rightarrow a_2 \rightarrow t$ will be shortest, and guarantees success in front-running messages between s and t .

8 CONCLUSION

Motivated by the increasing importance of latency in blockchain systems, in this work we have studied the empirical performance of strategic latency reduction methods as well as their theoretical limits. We formally defined the key notions of direct and triangular latencies. We have proposed a strategic scheme for reducing both types in a scheme called Peri and have shown its effectiveness experimentally on the Ethereum mainnet and an Ethereum testnet.

In this work, we have also explored the theory of strategic latency reduction in blockchain P2P networks. In a graph-based network model, we have shown that maximizing a notion of triangular-latency advantage is NP-hard. Even in this setting, however, we have shown via simulations that Peri achieves effective latency reduction. Finally, we have addressed the key question of whether it is possible to ensure strategy-proof peering protocols in unstructured blockchain P2P networks, and shown that it is in fact *impossible*: Agents can achieve direct connection to victims in low asymptotic time. Consequently, for any latency-sensitive application, blockchain P2P networks will *always* raise concerns.

ACKNOWLEDGEMENTS

We wish to thank Lorenz Breidenbach from Chainlink Labs and Peter van Mourik from Chainlayer for their gracious help in the setup for our direct-targeted-latency experiments.

G. Fanti and W. Tang acknowledge the Air Force Office of Scientific Research under award number FA9550-21-1-0090, as well as the generous support of Chainlink Labs and IC3. L. Kiffer contributed to this project while under a Facebook Fellowship.

REFERENCES

- [1] Gas and Fees. <https://ethereum.org/en/developers/docs/gas/>. (????). Accessed on April 29, 2022.
- [2] 2022. bloXroute Documentation. (2022). <https://docs.bloxroute.com/>.
- [3] 2022. Ethereum Networks Documentation. (2022). <https://ethereum.org/en/developers/docs/networks/>.
- [4] [Accessed Apr. 2022]. Blockchain on AWS. <https://aws.amazon.com/blockchain/>. ([Accessed Apr. 2022]).
- [5] [Accessed Apr. 2022]. BloXroute website. <https://bloxroute.com/>. ([Accessed Apr. 2022]).
- [6] [Accessed Apr. 2022]. Eth Gas Station. <https://ethgasstation.info/>. ([Accessed Apr. 2022]).
- [7] [Accessed Apr. 2022]. Ethereum Wire Protocol (ETH). <https://github.com/ethereum/devp2p/blob/master/caps/eth.md>. ([Accessed Apr. 2022]).
- [8] [Accessed Apr. 2022]. Fast Internet Bitcoin Relay Engine (FIBRE). <https://bitcoinfibre.org/>. ([Accessed Apr. 2022]).
- [9] [Accessed Apr. 2022]. Go Ethereum. <https://geth.ethereum.org/>. ([Accessed Apr. 2022]).
- [10] [Accessed Apr. 2022]. MEV-Explore v1. <https://explore.flashbots.net/>. ([Accessed Apr. 2022]).
- [11] Vijeth Aradhya, Seth Gilbert, and Aquinas Hobor. 2022. OverChain: Building a robust overlay with a blockchain. *arXiv preprint arXiv:2201.12809* (2022).
- [12] Vivek Bagaria, Sreeram Kannan, David Tse, Giulia Fanti, and Pramod Viswanath. 2019. Prism: Deconstructing the blockchain to approach physical limits. In *Proceedings of the 2019 ACM SIGSAC Conference on Computer and Communications Security*. 585–602.
- [13] C.E. Bonferroni. 1936. *Teoria statistica delle classi e calcolo delle probabilità*. Seeber. <https://books.google.com/books?id=3CY-HQAACAAJ>
- [14] Kyle Croman, Christian Decker, Ittay Eyal, Adem Efe Gencer, Ari Juels, Ahmed Kosba, Andrew Miller, Prateek Saxena, Elaine Shi, Emin Gün Sirer, et al. 2016. On scaling decentralized blockchains. In *International conference on financial cryptography and data security*. Springer, 106–125.
- [15] Philip Daian, Steven Goldfeder, Tyler Kell, Yunqi Li, Xueyuan Zhao, Iddo Bentov, Lorenz Breidenbach, and Ari Juels. 2020. Flash boys 2.0: Frontrunning in decentralized exchanges, miner extractable value, and consensus instability. In *2020 IEEE Symposium on Security and Privacy (SP)*. IEEE, 910–927.
- [16] Christian Decker and Roger Wattenhofer. 2013. Information propagation in the bitcoin network. In *IEEE P2P 2013 Proceedings*. IEEE, 1–10.
- [17] Sergi Delgado-Segura, Cristina Pérez-Solà, Jordi Herrera-Joancomartí, Guillermo Navarro-Arribas, and Joan Borrell. 2018. Cryptocurrency networks: A new P2P paradigm. *Mobile Information Systems* 2018 (2018).
- [18] Olive Jean Dunn. 1961. Multiple Comparisons among Means. *J. Amer. Statist. Assoc.* 56, 293 (1961), 52–64. <https://doi.org/10.1080/01621459.1961.10482090> arXiv:https://www.tandfonline.com/doi/pdf/10.1080/01621459.1961.10482090
- [19] Giulia Fanti and Pramod Viswanath. 2017. Deanonimization in the bitcoin P2P network. *Advances in Neural Information Processing Systems* 30 (2017).
- [20] Juan Garay, Aggelos Kiayias, and Nikos Leonardos. 2015. The bitcoin backbone protocol: Analysis and applications. In *Annual international conference on the theory and applications of cryptographic techniques*. Springer, 281–310.
- [21] Yilin Han, Chenxing Li, Peilun Li, Ming Wu, Dong Zhou, and Fan Long. 2020. Shrec: Bandwidth-efficient transaction relay in high-throughput blockchain systems. In *Proceedings of the 11th ACM Symposium on Cloud Computing*. 238–252.
- [22] Ethan Heilman, Alison Kendler, Aviv Zohar, and Sharon Goldberg. 2015. Eclipse attacks on bitcoin’s peer-to-peer network. In *24th {USENIX} Security Symposium ({USENIX} Security 15)*. 129–144.
- [23] Sebastian Henningsen, Daniel Teunis, Martin Florian, and Björn Scheuermann. 2019. Eclipsing ethereum peers with false friends. In *2019 IEEE European Symposium on Security and Privacy Workshops (EuroS&PW)*. IEEE, 300–309.
- [24] Richard M Karp. 1972. Reducibility among combinatorial problems. In *Complexity of computer computations*. Springer, 85–103.
- [25] William H. Kruskal and W. Allen Wallis. 1952. Use of Ranks in One-Criterion Variance Analysis. *J. Amer. Statist. Assoc.* 47, 260 (1952), 583–621. <http://www.jstor.org/stable/2280779>
- [26] Chenxin Li, Peilun Li, Dong Zhou, Zhe Yang, Ming Wu, Guang Yang, Wei Xu, Fan Long, and Andrew Chi-Chih Yao. 2020. A decentralized blockchain with high throughput and fast confirmation. In *2020 {USENIX} Annual Technical Conference ({USENIX} {ATC} 20)*. 515–528.
- [27] Jinyang Li. 2005. *Routing tradeoffs in dynamic peer-to-peer networks*. Ph.D. Dissertation. Massachusetts Institute of Technology.
- [28] Igor Makarov and Antoinette Schoar. 2020. Trading and arbitrage in cryptocurrency markets. *Journal of Financial Economics* 135, 2 (2020), 293–319.
- [29] Yifan Mao, Soubhik Deb, Shaileshh Bojja Venkatakrishnan, Sreeram Kannan, and Kannan Srinivasan. 2020. Perigee: Efficient peer-to-peer network design for blockchains. In *Proceedings of the 39th Symposium on Principles of Distributed Computing*. 428–437.
- [30] Petar Maymounkov and David Mazières. 2002. Kademlia: A peer-to-peer information system based on the xor metric. In *International Workshop on Peer-to-Peer Systems*. Springer, 53–65.
- [31] Adam Meyerson and Brian Tagiku. 2009. Minimizing average shortest path distances via shortcut edge addition. In *Approximation, Randomization, and Combinatorial Optimization. Algorithms and Techniques*. Springer, 272–285.
- [32] Andrew Miller, James Litton, Andrew Pachulski, Neal Gupta, Dave Levin, Neil Spring, and Bobby Bhattacharjee. 2015. Discovering bitcoin’s public topology and influential nodes. *et al* (2015).
- [33] Ahmed Afif Monrat, Olov Schelén, and Karl Andersson. 2019. A survey of blockchain from the perspectives of applications, challenges, and opportunities. *IEEE Access* 7 (2019), 117134–117151.
- [34] Gleb Naumenko, Gregory Maxwell, Pieter Wuille, Alexandra Fedorova, and Ivan Beschastnikh. 2019. Erelay: Efficient transaction relay for bitcoin. In *Proceedings of the 2019 ACM SIGSAC Conference on Computer and Communications Security*. 817–831.
- [35] A. Osipovich. 1 Apr. 2021. High-Frequency Traders Eye Satellites for Ultimate Speed Boost. *Wall Street Journal* (1 Apr. 2021).
- [36] A. Osipovich. 15 Dec. 2020. High-Frequency Traders Push Closer to Light Speed With Cutting-Edge Cables. *Wall Street Journal* (15 Dec. 2020).
- [37] Elias Rohrer and Florian Tschorsch. 2019. Kadcad: A structured approach to broadcast in blockchain networks. In *Proceedings of the 1st ACM Conference on Advances in Financial Technologies*. 199–213.
- [38] Tim Roughgarden. 2020. Transaction fee mechanism design for the Ethereum blockchain: An economic analysis of EIP-1559. *arXiv preprint arXiv:2012.00854* (2020).
- [39] Avron Shane. 2021. Advantages and Disadvantages of a Peer-to-Peer Network. *Flevy Blog* (2021).

- [40] Bhavesh Toshniwal and Kotaro Kataoka. 2021. Comparative Performance Analysis of Underlying Network Topologies for Blockchain. In *2021 International Conference on Information Networking (ICOIN)*. IEEE, 367–372.
- [41] Aaron Van Wirdum. 2016. HOW FALCON, FIBRE AND THE FAST RELAY NETWORK SPEED UP BITCOIN BLOCK PROPAGATION (PART 2). *Bitcoin Magazine* (2016).
- [42] Taotao Wang, Chonghe Zhao, Qing Yang, Shengli Zhang, and Soung Chang Liew. 2021. Ethna: Analyzing the Underlying Peer-to-Peer Network of Ethereum Blockchain. *IEEE Transactions on Network Science and Engineering* 8, 3 (2021), 2131–2146.
- [43] Wenbo Wang, Dinh Thai Hoang, Peizhao Hu, Zehui Xiong, Dusit Niyato, Ping Wang, Yonggang Wen, and Dong In Kim. 2019. A survey on consensus mechanisms and mining strategy management in blockchain networks. *Ieee Access* 7 (2019), 22328–22370.
- [44] Haifeng Yu, Ivica Nikolić, Ruomu Hou, and Prateek Saxena. 2020. Ohie: Blockchain scaling made simple. In *2020 IEEE Symposium on Security and Privacy (SP)*. IEEE, 90–105.

A APPENDIX

A.1 Proofs

A.1.1 Proof of Theorem 6.1. It is known that the set cover problem is NP-complete [24]. We take an arbitrary instance of the set cover problem:

PROBLEM 2. Given a finite set of elements $\Sigma = \{\sigma_1, \dots, \sigma_p\}$ and its subsets $\Gamma_1, \dots, \Gamma_q$. We aim to find the fewest collection of subsets from $\Gamma_{1:q}$, whose union equals Σ .

We construct a graph $G = (\mathcal{V}, \mathcal{E})$ as below. Each element σ_i in Σ corresponds to a unique node of the same name. Each subset Γ_j corresponds to 2 nodes γ_j^+, γ_j^- . Finally, a fresh node c is added. In other words, $\mathcal{V} = \{c\} \cup \bigcup_{i=1}^p \{\sigma_i\} \cup \bigcup_{j=1}^q \{\gamma_j^+, \gamma_j^-\}$.

For each pair $(i, j) \in [p] \times [q]$, edge $(\sigma_i, \gamma_j^-) \in \mathcal{E}$ if and only if $\sigma_i \in \Gamma_j$. Besides these, \mathcal{E} contains (γ_j^-, γ_j^+) and (γ_j^+, c) for each j . Fig. 5 illustrates an example of topology of G .

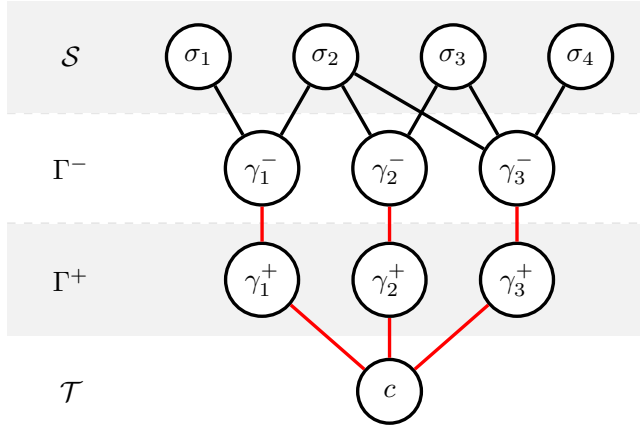


Figure 5: Topology of G given a set cover instance where $\Gamma_1 = \{\sigma_1, \sigma_2\}$, $\Gamma_2 = \{\sigma_2, \sigma_3\}$ and $\Gamma_3 = \{\sigma_2, \sigma_3, \sigma_4\}$.

We take set of sources $\mathcal{S} \triangleq \{\sigma_1, \sigma_2, \dots, \sigma_p\}$ and set of destinations $\mathcal{T} \triangleq \{c\}$. As expected, the original distance $d_G(s, c) = 3$ for each $s \in \mathcal{S}$. Now we claim that if we can solve Problem 1 in polynomial time for $G, \mathcal{S}, \mathcal{T}$ where $\forall e \in \mathcal{E}$ ($w(e) = 1$), $\tau = 1.99$ (breaking ties) and $k \in [2, 1+q]$, then we can also solve the original set cover problem in polynomial time.

When $k \in [2, 1+q]$, we are able to select k spy nodes amongst nodes in \mathcal{V} . The optimal choice must

- contain c : Otherwise, there must exist a spy node in Γ^+ , or the placement will not be effective at all. Replacing this spy node with c will not decrease the advantage.
- contain only nodes in Γ^- other than c : If σ_i is chosen, then this spy node serves no other pair than (σ_i, c) . We pick j where $\sigma_i \in \Gamma_j$ and choose γ_j^- instead. This will not decrease the advantage. If γ_j^+ is chosen, then it benefits the advantage by moving it to γ_j^- , even when this creates duplicates.

Therefore, to solve the advantage maximization, we are essentially picking nodes in Γ^- , which corresponds to picking subsets among $\Gamma_1, \dots, \Gamma_q$. If we can solve the advantage maximization in polynomial time for all $k \in [2, q+1]$, we can enumerate all solutions and pick the smallest k where the advantage reaches p , the total number of elements in \mathcal{S} , and also the best advantage we have between \mathcal{S} and $\mathcal{T} = \{c\}$. This also solves the minimum set cover problem known to be NP-hard, which is a contradiction. Therefore, Problem 1 is NP-hard, and such polynomial-time algorithm exists only if $P = NP$. ■

A.1.2 Proof of Proposition 6.2. We present the counter-example in Fig. 6, which is a tree with $2k+1$ branches. In this tree, the initial pair of nodes chosen by the greedy algorithm must be g and h_i for some $i \in [k]$, because a shortcut between them puts 3 pairs at maximum of sources and destinations $\{(g, t_{3i-j}) | j \in \{0, 1, 2\}\}$ under the risk of being front-run. At each of the following steps, the greedy algorithm will have to continue choosing an additional peer from $\{h_i | i \in [k]\}$, which further increases the advantage by 3. Hence, with 2ℓ peers where $\ell < k/2$ is an integer, the total advantage equals $6\ell - 3$.

However, these 2ℓ peer connections can be put to better uses. If we choose $\{s_1, \dots, s_\ell\} \cup \{r_1, \dots, r_\ell\}$ instead, then the shortcut pairs of sources and destinations can be described by $P = \{(s_i, r_j) | i \neq j, i \in [\ell], j \in [\ell]\}$, where $|P| = \ell(\ell-1)$. Therefore, the ratio of the greedy algorithm solution to the maximum advantage is at most $\frac{6\ell-3}{\ell(\ell-1)} \sim \frac{6}{\ell}$, which can be arbitrarily close to 0 as ℓ, k become arbitrarily large. Equivalently, the greedy algorithm cannot guarantee an α -approximately optimal solution for any $\alpha > 0$. ■

A.1.3 Proof of Theorem 7.2. We first show the result for a single target, i.e., $|U| = 1$. Let a denote an adversarial node and x denote the message sender (that is, $U = \{x\}$). We let the adversary perform the following 3-step strategy iteratively.

- Step 1. Wait Δ_1 for the first arrival of a new message M sent by x .
- Step 2. Keep only the peer that contributed to the first arrival, and get $d-1$ random new addresses from the oracle to replace the other peers. The probability of x belonging in these addresses is lower-bounded by $q > 0$. Send peering requests repeatedly until a peer slot becomes available.

If x is already one of the neighbors at Step 1, it will surely be kept in Step 2 because $w(x, a)$ is already the shortest path length between x and a on the network, implied by the triangle inequality (8). In the end, it will remain a peer of the adversary. Because the samplings for replacement nodes are independent across K iterations, we can geometrically decrease the probability that x is missed in the entire

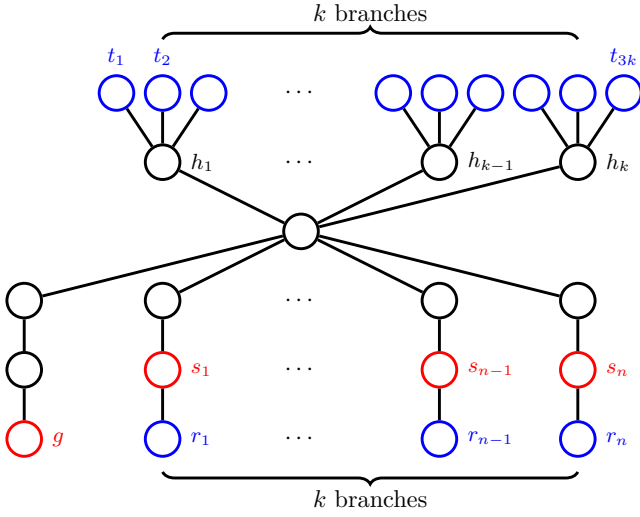


Figure 6: Greedy algorithm cannot maximize advantage with proximity greater than 0. $\tau = 3.99$. Red nodes are sources and blue nodes are destinations.

procedure by increasing K . This intuitively explains why K is of order $O(\log \varepsilon^{-1})$. Next, we make this intuition precise.

Let

$$K \triangleq \frac{\log(\varepsilon/2)}{\log(1-q)}, \quad \varepsilon_1 = \varepsilon_2 \triangleq \frac{\varepsilon \log(1-q)}{4 \log(\varepsilon/2)}.$$

In Step 1, it is desired that the sender sends at least 1 message during the time window of length Δ_1 with probability at least $1 - \varepsilon_1$.

We will use the following lemma, which states that it is highly probable that during a sufficiently long window of time, a node broadcasts at least γ messages every unit of time on average.

LEMMA A.1. *A Poisson process $\{M_u(t), t \geq 0\}$ with rate ν satisfies that there exist constants $\gamma, \mu > 0$, such that*

$$\mathbb{P}[M_u(t + \Delta) - M_u(t) < \gamma\Delta] < \frac{\mu}{\Delta}, \quad \forall t, \Delta > 0.$$

By Assumption (II) from Definition 7.1 and Lemma A.1, there exist constants μ, γ such that

$$\mathbb{P}[M_x(t + \Delta_1) - M_x(t) \geq \gamma\Delta_1] \geq 1 - \frac{\mu}{\Delta_1}.$$

Here by taking $\Delta_1 = \max\{\gamma^{-1}, \mu\varepsilon_1^{-1}\}$, we obtain the lower-bound probability that x broadcasts at least 1 message during any time interval of length at least Δ_1 .

In Step 2, we would like to wait Δ_2 for all the $d - 1$ new nodes being connected to the adversary. This requires each new node to have at least 1 free slot. We consider the worst case where none of the slots are free in the beginning. For each target peer p , each one of the f slots will become free after a period of time T_0 , where $T_0 \sim \text{Exp}(\lambda)$. Since one slot is already sufficient, the probability the peer p becomes available after Δ_2 is lower-bounded by $1 - e^{-\lambda\Delta_2}$.

This expression is further lower-bounded by $1 - \frac{\zeta}{\Delta_2}$ for $\zeta = \frac{1}{e\lambda}$.

Then, considering all the $(d - 1)$ peers, we may use the union bound to derive a lower bound of the probability P_3 that all the

$d - 1$ peers are available.

$$P_3 \geq 1 - \frac{(d-1)\zeta}{\Delta_2}.$$

We want P_3 to be at least $1 - \varepsilon_2$. This can be achieved by letting

$$\Delta_2 = \frac{(d-1)\zeta}{\varepsilon_2}.$$

After taking K iterations of these steps, the probability of finding x equals $1 - (1 - q)^K$, while the probability that all executions of Steps 1 & 3 are successful is at least $1 - K\varepsilon_1 - K\varepsilon_2$. The overall probability equals

$$\begin{aligned} [1 - (1 - q)^K] (1 - K\varepsilon_1 - K\varepsilon_2) &\geq 1 - (1 - q)^K - K(\varepsilon_1 + \varepsilon_2) \\ &= 1 - \frac{\varepsilon}{2} - \frac{\varepsilon}{2} \\ &= 1 - \varepsilon. \end{aligned}$$

On the other hand, the total time consumption equals

$$\begin{aligned} K\Delta_1 + K\Delta_2 &= O(\log \varepsilon^{-1}) \left[O(\varepsilon^{-1} \log \varepsilon^{-1}) + O(\varepsilon^{-1}) \right] \\ &= O(\varepsilon^{-1} \log^2(\varepsilon^{-1})). \end{aligned} \quad (9)$$

Next, we show how to extend this result to an arbitrary U via a union bound.

From (9), we know that with probability $1 - \varepsilon/|U|$, the adversary is able to find the network ID of an arbitrary node $u \in U$ within time

$$O\left((\varepsilon/|U|)^{-1} \log^2(\varepsilon/|U|)\right) = O\left(|U| \varepsilon^{-1} \log^2(\varepsilon^{-1})\right).$$

Regardless of how the adversary allocates time to the tasks of finding each $u \in U$, the probability of finding all of them is at least $1 - |U| \times \varepsilon/|U| = 1 - \varepsilon$ by the union bound. As for the time consumption, we consider the worst case where the agent has to run the algorithms for finding each $u \in U$ sequentially. In this case, the total time consumption is the time consumption above of each single task multiplied by number of tasks $|U|$, which equals

$$O\left(|U|^2 \varepsilon^{-1} \log^2(\varepsilon^{-1})\right). \quad \blacksquare$$

A.1.4 Proof of Proposition 7.3. First of all, we assume N , the number of nodes, to be upper-bounded so that the probability q that the oracle returns a target after a single draw satisfies $0 < q_1 \leq q \leq q_2 < 1$ for some constants q_1, q_2 . In order to connect to the target, it is necessary for the adversary to draw it using the oracle. Temporarily, we ignore the other necessary steps (such as judging if an existing peer is the target) and consider only drawing nodes. Then, the probability P that the target is drawn within K steps satisfies

$$1 - (1 - q_1)^K \leq P \leq 1 - (1 - q_2)^K.$$

To let $P = 1 - \varepsilon$, we should equivalently have $K = \Theta(\log \varepsilon^{-1})$ because

$$\frac{\log \varepsilon}{\log(1 - q_2)} \leq K \leq \frac{\log \varepsilon}{\log(1 - q_1)}.$$

Considering that each drawing takes $\Theta(1)$ time, it takes at least $\Theta(K) = \Theta(\log \varepsilon^{-1})$ time to find the target with the oracle w.p. at least $1 - \varepsilon$. As argued above, drawing the target is a necessary condition for the final peer connection to it. Hence, $\Omega(\log \varepsilon^{-1})$ is a lower bound of time consumption. \blacksquare

A.1.5 Proof of Lemma A.1. Let ν denote the arrival rate. For any Δ , we assign $k = \nu\Delta/2$, and obtain

$$\begin{aligned}
\mathbb{P}\left[M_u(t + \Delta) - M_u(t) < \frac{\nu\Delta}{2}\right] &= e^{-\nu\Delta} \sum_{i=0}^{\lfloor \nu\Delta/2 \rfloor} \frac{(\nu\Delta)^i}{i!} \\
&\sim e^{-2k} \sum_{i=0}^k \frac{(2k)^i}{i!} \\
&\lesssim ke^{-2k} \sup_{t \in [0, k]} \frac{(2k)^t}{t!} \\
&\lesssim ke^{-k} \\
&\lesssim \frac{1}{k} \sim \frac{1}{\nu\Delta}.
\end{aligned} \tag{*}$$

This already justifies the claim. It remains to prove (*). By Stirling's approximation, let

$$f(t) = \log \frac{(2k)^t}{t!} \approx t \log(2k) - \frac{\log t}{2} - t \log t + t.$$

As a result,

$$f'(t) \approx \log(2k) - \frac{1}{2t} - \log t.$$

As $\log t + 1/(2t)$ monotonically increases in $(1/2, \infty)$, we may assert that the maximizer τ satisfies

$$f'(\tau) = 0 \iff 2k = \tau e^{\frac{1}{2\tau}}.$$

It can be confirmed that $\tau \in [0, k]$. Hence,

$$\sup_{t \in [0, k]} \frac{(2k)^t}{t!} \sim \frac{(\tau e^{\frac{1}{2\tau}})^\tau}{\sqrt{\tau} \tau^\tau e^{-\tau}} \lesssim e^\tau \lesssim e^k. \quad \blacksquare$$

A.2 Evaluation of direct targeted latency over Ethereum Mainnet

We ran limited experiments on targeted latency by measuring transactions from a target / victim node in Germany operated by Chainlink ; the node sends 2 transactions per hour on average. These transactions originate from an account (Ethereum address) exclusive to the victim node, i.e., all transactions are sent only by the victim. The node kept running on the network during our experiments.

We evaluate each of the four methods from §5.1.1, measuring both their ability to reduce targeted latency and their ability to connect to (i.e., infer) the IP address of our target node on the Ethereum main P2P network. To this end, we establish 4 EC2 instances in the ap-southeast-1 AWS data center in Singapore, which have a 160 ms round-trip time to Germany. They are located within the same subnet as a public bloXroute relay. As in §5.1, we deploy a full Go-Ethereum node on each host with at most 50 peers. The proportion of outbound peers remain the same. We conduct the experiments under the same procedure and take similar anti-biasing measures, except for three key differences. First, we define the relevant transactions as only those sent by the target's account. Second, we set the Peri period to 30 minutes to match the frequency of source transactions. Third, the duration of each experiment is extended from 8 hours to 16 hours to permit a larger number of Peri periods.

We ran 23 experiments from March 19, 2022 to April 19, 2022. The Hybrid and Baseline clients were able to establish connections

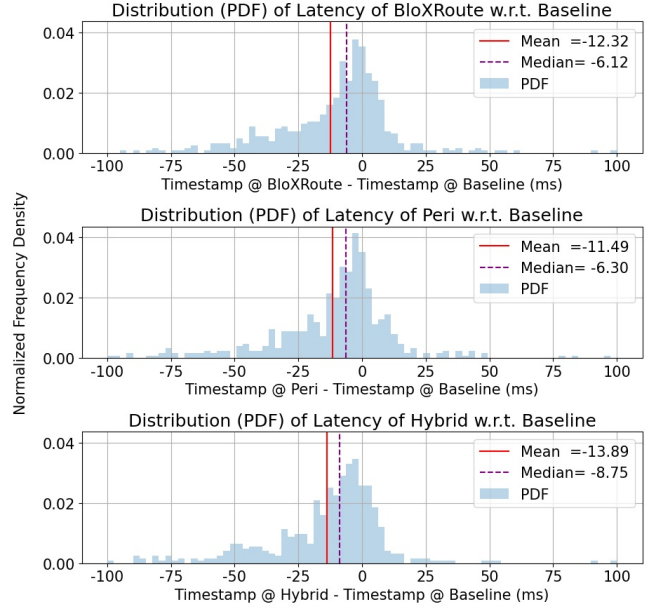


Figure 7: PDFs of distributions of targeted latency.

to the victim node once each. The distributions of targeted latency of each method are displayed in Fig. 7. In total, we analyzed the latencies of 654 transactions.

Over distributions in Fig. 7, we performed Kruskal-Wallis test and obtained p-value = 0.0235, which allows us to reject the null hypothesis at significance level 5% and continue with a Dunn's test. Then, we performed Dunn's test with Bonferroni correction over these distributions. The p-values are listed in Table 3. At significance level 5%, we cannot assert a difference between the means of any pair of distributions. This indicates that all the methods share a similar ability to reduce direct targeted latency. We can further observe this phenomenon from Fig. 7, where they share a similar ability to reduce direct targeted latency by 14% to 18% of the end-to-end delay, and the hybrid method outperforms the other two methods with a slight advantage. Unlike reduction of direct global latency, the Peri algorithm is no longer significantly worse than the bloXroute relay network at reducing direct targeted latency, which makes it a free replacement of bloXroute services for agents with specific targets. An agent with bloXroute services can also further boost the latency reduction by an additional 13% by stacking the Peri algorithm and turning hybrid. In addition, Peri can potentially help an agent identify the IP address of a victim, while bloXroute, which intermediates connections, cannot support such functionality.

Pair	(B, P)	(B, H)	(P, H)
p-value	1.0	0.0532	0.0529

Table 3: Pairwise p-values of Dunn's test over distributions of targeted latency in Fig. 7, comparing bloXroute (B), Peri (P), and Hybrid (H).

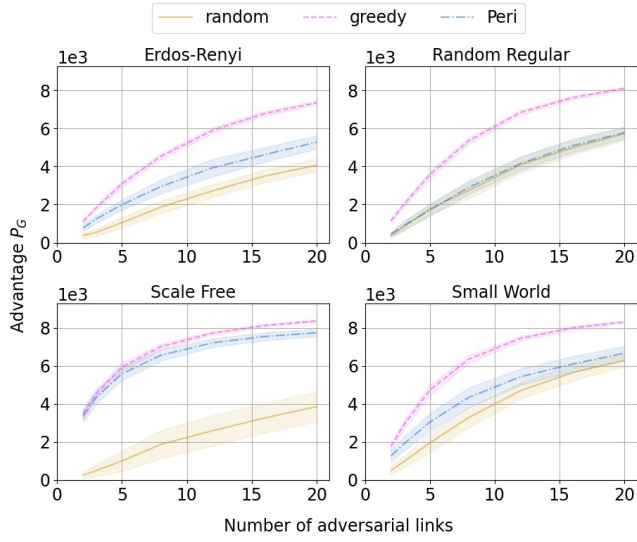


Figure 8: Advantage-Peer-count curves on original random graph models. The mean of the curves are shown by solid lines, and the standard deviations are shown by the transparent color zones centered at the mean.

A.3 Simulations of Advantage Maximization Algorithms on Original Topologies

We synthesize the network models as in §6.2 without centralizing them by introducing hub nodes. We reuse other setups in the original simulation, and plot the advantage-peer-count curves in Fig. 8.

For all the graph models, both Peri and Greedy achieve a higher advantage A_N than the random baseline, with Greedy outperforming Peri by varying amounts. For the most decentralized models, such as the random regular and small world, the advantage of Peri is much closer to that of random baseline than the greedy algorithm. On the other hand, for models with a few high degree nodes (i.e., hubs), Peri inserts shortcut peering connections almost as well as the greedy algorithm, in spite of its limited knowledge of the graph. Therefore, the performance of Peri is likely to be stronger on networks with many hubs. This is consistent with our conclusion in §6.2.